CHAPTER 49

RESEARCHES ON STEEL-PIPE BREAKWATER

S. Nagai

Professor of Hydraulic Engineering,
Department of Civil Engineering,
Faculty of Engineering,
Osaka City University,
Osaka, Japan.

INTRODUCTION

As a new type of vertical-wall breakwater built in soft ground a breakwater, composed of a single row of large steel pipes with diameters of some 1.5 to 3.0 meters driven into a sea bottom, has been proposed for the water areas where are not directly exposed to a great ocean. Experiments for the fundamental study were conducted in the medium wave channel of the hydraulic laboratory in Osaka City University, and model experiments were performed for practical design of the steel pipe breakwater planned to build in the Port of Osaka at a 1/10 scale in the large wave tank in the Field Hydraulic Laboratory.

PART I, FUNDAMENTAL STUDY

EXPERIMENTAL EQUIPMENT AND PROCEDURES

The experiments were performed in the medium wave channel, 25m long, 2.0m wide and 1.2m deep, and the model breakwater was composed of a single row of steel pipes with a diameter of 10cm which were fixed perpendicular to the bottom of the wave channel in close contact with each other, as seen in Fig. 1. Waves were generated by a flutter-type wave generating machine located at the counter-side to the model breakwater in the channel, and the periods, heights and lengths of the waves used in the experiments were T_m = 1.23sec to 1.8sec, H_m = 13cm to 20cm and L_m = 200cm to 300cm in the water depths h_m = 40cm to 60cm. If the model-to-prototype scale is taken as 1/15, the diameter of the pipe, the characteristics of the waves and the water depths used in the experiments would be equivalent in prototype to D_p = 1.5m, T_p = 4.7sec to 8.0sec, H_p = 2m to 3m, L_p = 30cm to 60cm, h_p = 6m to 9m respectively.

The pressures of the waves exerted on the steel-pipe breakwater were measured at the top-face and side of the steel pipe, as shown in Fig. 2, by the simultaneous use of six pressure gauges of strain-guage type, and the wave pressures exerted on a breakwater with a plain vertical wall were also measured in the same characteristics of waves and water depths as those used in the tests of the steel-pipe breakwater for the comparison between them. The resultant of the wave pressures exerted on one steel pipe was measured by the measurement of moments at two points on the pipe (Figs. 21, 22) in order to check the resultant of the wave pressures obtained by the vertical distribution curves of the pressures recorded on the six pressure gauges.

The heights of the waves were recorded just in front of the breakwater and at distances of 5.5m and 7.0m offshore from the breakwater by use of three wave recorders of strain-gauge type.

WAVE PRESSURES EXERTED ON THE STEEL-PIPE BREAKWATER

WAVE PRESSURES ON THE TOP-FACE OF THE STEEL-PIPE

a) BREAKWATER WITHOUT A RUBBLE MOUND

The intensities of wave pressures and their vertical distributions on the top face of the circular steel pipe are illustrated in Figs. 3a, 4a, 5a, 6a, 7a and 8a, in comparison with those of the breakwater with a plain vertical wall. In these figures P_e denotes the resultant of the wave pressures measured on the top face of the pipe, P_S is the resultant wave pressure calculated by Sainflou's simplified method which is obtained by

$$P_S = \frac{1}{2} W_0 \, (H + \delta_0 + h) \left(h + \frac{H}{\cosh mh}\right)$$

where $\delta_0 = \dfrac{\pi H^2}{L} \coth mh$, $m = \dfrac{2\pi}{L}$, and W_0 defines the unit weight of water.

P_c is the resultant pressure calculated by the following equation derived from the small amplitude wave theory

$$P_c = \frac{1}{2} W_0 \, (h^2 - H^2) + W_0 H \left\{ h + H + \frac{\sinh (h + H)}{m \cosh mh} - (h + H) \frac{\cosh m(h + H)}{\cosh mh} \right\},$$

and P_A is the resultant pressure calculated by the equation of maximum simultaneous pressure proposed by the author for standing waves in shallow water, $h/L \leqq 0.35$,

$$P_A = \frac{1}{2} W_0 \, (h^2 + H^2) + W_0 \frac{H}{m} \tanh mh$$

Figs. 3b, 4b, 5b, 6b, 7b and 8b show the behaviors of the waves in front of the vertical walls in Figs. 3a, 4a, 5a, 6a, 7a and 8a respectively.

As seen in Figs. 3b to 8b, the crests of the waves slightly break on the vertical wall of steel pipes, causing small increase in the intensities of pressure around the still water surface.

Accordingly the resultants of wave pressures exerted on the steel-pipe breakwater were 3 to 24 per cent larger than those on the plain vertical wall. The vertical distributions of the pressures measured and the resultants of those pressures are in comparatively good agreement with those calculated by the equation (A), being the ratioes between Pe and P_A , $Pe/P_A = 0.84$ to 0.88 for the plain vertical wall, and $Pe/P_A = 0.94$ to 1.00 for the steel-pipe breakwater. This result indicates that the concentration of wave energy into the concave part between the two adjacent circular pipes is not considerable in the steel-pipe breakwater used in these experiments while it was much larger in vertical-wall breakwaters which were constructed with larger cells 10m to 15m in diameter. The characteristics of the waves tested and the resultants of the wave pressures which were measured and calculated are listed in Table 1.

b) BREAKWATER WITH A RUBBLE MOUND

Although a rubble mound will be considered to be built at the harbor-and sea-sides of a steel-pipe breakwater in order to reduce the deflections of the steel pipe at the sea-bottom, it was clearly proven by the experiments that the construction of the base-rubble mound made waves break and increased the pressures of the waves exerted on the steel pipes, creating sometimes shock pressures of comparatively large intensity. The effect of the rubble mound on the wave pressures exerted on the steel-pipe breakwaters as well as on the plain vertical walls are shown in Figs. 9 ~ 14, and Figs. 15 ~ 20 show the behaviors of the waves in front of the steel-pipe breakwaters in the cases of Figs. 9 ~ 14 respectively. The experimental data are listed in Table 2.

The resultants of the wave pressures exerted on the steel-pipe breakwater with a rubble mound were also 2 to 36 per cent larger than those on the plain vertical wall with a rubble mound, and as the water depth on the rubble mound, h_1 , decreases, the pressures of waves increase, following shock pressures of comparatively large intensity, the vertical distributions of which are similar to the A-type of high shock pressures[1], when h_1/H are 1.3 to 1.4 or little less.

WAVE PRESSURES ON THE SIDES OF THE STEEL-PIPE

The pressures of waves exerted on the sides of the steel pipe were measured at the points with an angle 47 degrees to the direction of the oncoming wave, as shown in Fig. 2, in the steel-pipe breakwaters without and with a rubble mound. The data of these experiments are summarized in Tables 3 and 4.

(1) Nagai, S., "Shock Pressures Exerted by Breaking Waves on Breakwaters", Proc. A.S.C.E., Waterways and Harbors Division, Vol. 86, June 1960.

From Tables 3 and 4 it is noted that the wave pressures exerted on the side of the pipe are a little larger in many cases of the experiments than those on the top face of the pipe, while the former show a little smaller values than the latter in the three cases of the experiments. Accordingly it may be said that there is seen no distinguished concentration of wave energy into the concave part between the two adjacent circular pipes in the vertical breakwater composed of a single row of steel pipes with a diameter of 1.5m in the wave conditions used in these experiments.

WAVE PRESSURES EXERTED ON ONE STEEL PIPE OF THE STEEL-PIPE BREAKWATER

A steel pipe with the same diameter of 10cm as that of the steel pipes of the breakwater was suspended from a fixed point located over the wave channel at the middle part of the breakwater, as seen in Figs. 21 and 22. Moments exerted by the oncoming waves were measured at the points of G_1 and G_2 in Fig.22. The resultant of the pressures, P_x, on the steel pipe and the point of application of the resultant pressure, l_x, were calculated by

$$P_x = \frac{M_1 - M_2}{l} \qquad \text{and} \qquad l_x = \frac{M_2}{M_1 - M_2} l$$

P_x were compared with the resultant pressures, P_{me}, obtained by the vertical distribution curves of pressures measured on the top face of the steel pipe and those calculated by the equation (A), P_{mA}. Those data are listed in Table 5.

From Table 5 it is noted that P_x are 13 to 23 per cent larger than P_{me}. In view of the result that the resultant pressures on the sides of the pipe are a little larger, up to 14 per cent, than those on the top face of the pipe, the values of P_x may be said probably correct.

PART II. MODEL STUDY OF THE STEEL-PIPE BREAKWATER IN THE PORT OF OSAKA

MAIN PURPOSES OF THE EXPERIMENT

The steel-pipe breakwater composed of a single row of 60 steel pipes with a diameter of 2 meters was decided to be built at the entrance of the North Harbor (entrance width = 160m) in the Port of Osaka when our fundamental study had been performed, and the model experiments were conducted in the large wave tank for the steel-pipe breakwater which was under design to be built in the Port of Osaka.

The main purposes of this model experiment were: (1) Measurements of the wave pressures and their vertical distributions on the steel pipe as well as of the sheltering effect of the breakwater when the steel pipes are driven at some 5 to 10cm space between the adjacent pipes; (2) finding the way of reconstruction after destructions of part of the breakwater due to the collision of drifting ships during typhoons.

EXPERIMENTAL EQUIPMENT AND PROCEDURES

The model experiments were performed at a 1/10-model-to-prototype scale in the large wave tank, 60m long, 10m wide and 2.5m deep. The model steel pipes with a diameter of 20cm were fixed perpendicular to the bottom of the tank at an constant space of one cm between the adjacent pipes (Fig. 24), and the tops of the pipes were fixed in some experiments and free in other experiments in which the deflections of the top were measured (Fig. 26).

The heights of the oncoming waves were measured by two wave-recorders located at 10m and 13m seaward from the breakwater and the heights of the waves transmitted to harbor-side through the spaces between the pipes were measured at 3m and 6m distances from the breakwater (Fig. 23), in two cases when the one-cm-spaces between the pipes ran entirely from the top to the bottom of the pipe and the spaces above the low water level were shut off waves passing into the harbor basin by iron plates welded to the both sides of the pipes. (Fig. 27)

The characteristics of waves used in the experiments were Tm (period) = 1.58sec to 2.20sec, Tp (period in prototype) = 5.0sec to 7.0sec, and Hm (height) = 17.7cm to 30cm, Hp (height in prototype) = 1.77m to 3.0m. The kinds of the experiments performed are listed in Table 6.

EXPERIMENTAL RESULTS AND SOME CONSIDERATIONS

FIXED TOPS OF STEEL PIPES WITH SHELTER-PLATES

The experimental results are summarized in Table 7(a) when the tops of the steel pipes were fixed and all the spaces between the adjacent pipes were shut up with shelter-plates from the low water level to the top of the pipe, the heights of which were changed 17cm and 36cm above the low water level, that is, D.L. + 5.0m and + 7.0m above the datum low water level in prototype.

The intensities of pressures exerted on the top face and side of the pipe as well as their vertical distributions in Runs No. 1 and 6 are shown in Fig. 28, and those in Runs No. 5 and 10 shown in Fig. 29. The behaviors of the waves around the breakwater are shown in Figs. 30(a), 30(b), 31(a) and 31(b).

The ratioes of the resultant pressures between on the top face and side of the pipe are 0.99 to 1.16, and these ratioes are nearly same as those of 0.94 to 1.14 obtained in the fundamental experiments in which steel pipes were stood close together.

MOVABLE TOPS OF STEEL PIPES WITH SHELTER-PLATES

When the tops of the steel pipes were deflected up to 2cm at the tops, the pressures exerted on the pipes decreased slightly on the top face of the pipe but those on the side increased slightly, and the ratioes between the resultant pressures on the top face of the pipe and calculated by the equation(A), P_A, were 0.63 to 1.08, as well as the ratioes of the resultant pressures between on the side and top face of the pipe were 1.19 to 1.89. These experimental data are listed in Table 7(b).

FIXED TOPS OF STEEL PIPES WITHOUT SHELTER-PLATES

When the tops of the steel pipes were fixed and all the shelter-plates were taken off to make waves freely transmit into the harbor basin through the one-cm spaces between the adjacent pipes, the pressures on the top of the pipe decreased some 10 per cent compared with those in the breakwater with the shelter-plates, but the pressures on the side of the pipe did not decrease. The main reason is considered due to the concentration of wave energy into the spaces. The experimental results are listed in Table 7(c). The pressure distribution curves on the top and side of the pipe in Runs No.3 and 6 in Table 7(c) are depicted in Fig. 32, and the behaviors of waves in those runs are shown in Figs. 33(a) and (b) respectively.

TRANSMISSION OF WAVES THRO' THE SPACES BETWEEN THE PIPES

If the diameter of the steel pipe and the space between the adjacent pipes are denoted by D and d, ratio, H_T/H_I, between the height of the wave transmitted through the spaces, H_T and that of the incoming wave, H_I, is obtained by

$$\frac{H_T}{H_I} = \sqrt{\frac{d}{D + d}}$$

Taking y the vertical distance to which the shelter-plate extends below the still water surface, the ratio, H'_T/H_I, of height of wave, H'_T, transmitted between the bottom and the depth y below the still water level, to the incoming wave height H_I is obtained for waves of small amplitude[2]

$$\frac{H'_T}{H_I} = \sqrt{\frac{d}{D + d}}\sqrt{\frac{\dfrac{4\pi(y + h)/L}{\sinh(4\pi h/L)} + \dfrac{\sinh 4\pi(y + h)/L}{\sinh(4\pi h/L)}}{1 + \dfrac{4\pi h/L}{\sinh(4\pi h/L)}}}$$

(2) Wiegel, Robert L., "Transmission of Waves Past A Rigid Vertical Thin Barrier", Proc. A.S.C.E., WWI, March, 1960.

where h is the water depth, and L denotes the wave length.

The results of comparisons between the experimental values of H_T/H_I and H'_T/H_I, theoretical values calculated by the two equations described above are shown in Tables 7(a), and (c). The comparisons show:

(1) When there was no overtopping of waves in the steel-pipe breakwater with the shelter-plates, the experimental values of H'_T/H_I are generally in good agreement with the calculated values. (Table 7(a)).

(2) When no overtopping of waves was seen in the steel-pipe breakwater without the shelter plates, the experimental values of H_T/H_I are 6 to 11 per cent larger than the calculated ones (Table 7(c)). This is due to the concentration of waves into the one-cm spaces between the adjacent circular pipes.

(3) When waves overtop over the top of the breakwater, the values of H_T/H_I and H'_T/H_I increase up to some 20 per cent.

(4) When the top of the breakwater without the shelter-plates oscillated with a maximum amplitude of 7cm, the experimental values of H_T/H_I were 26 to 37 per cent, which were little larger than those of the breakwater with fixed top.

EXPERIMENTS FOR RECONSTRUCTION

There was little anxiety about severe damages of the steel-pipe breakwater due to waves as the design wave was so small that $H_p = 2$ to 3m, $T_p = 5$ to 7sec. But a great possibility was considered to serious damages due to the collision of drifting ships during typhoons. As a way of reconstuction of part of the breakwater after the destructions, it was proposed to move the destructed part of the breakwater by some 2m seaward from the site of the breakwater and drive again steel pipes 2m in diameter into the sea-bottom there.

Several experiments in such situation of the breakwater were conducted to know any changes in wave pressures exerted on the steel pipes and waves transmitted into the harbor basin. It was proven from the experiments that there would be no remarkable increases in the wave pressures and the wave heights transmitted into the harbor basin. Figs. 34 and 35 show experiments concerned with the reconstructed part of the breakwater.

CONSTRUCTION OF THE BREAKWATER

The construction of the breakwater, which was composed of 60 steel pipes 2m in diameter, was started in July, 1965 in the Port of Osaka and completed at the end of May, 1966. The spaces between the adjacent steel pipes were some 5cm in average. Fig. 36 shows the steel-pipe breakwater in near completion, and Fig. 37 the breakwater undergoing horizontal load tests in May, 1966. Figs. 38 and 39 shows the breakwater after the completion.

ACKNOWLEDGMENTS

The writer wishes to express his appreciation to three assistants, Mr. S. Kubo, K. Oda, and K. Tokikawa, in the writer's laboratory for performing the laboratory experiments and for preparing the illustrations, and to Miss. Y. Ueno for typing the original manuscript.

Fig. 1. Model of the steel-pipe breakwater.

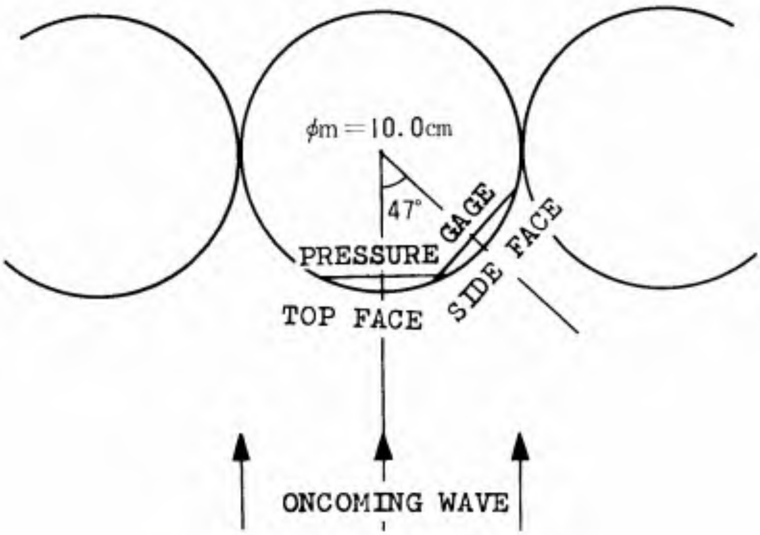

Fig. 2. Plan of the steel-pipe breakwater and locations of the pressure-gauges.

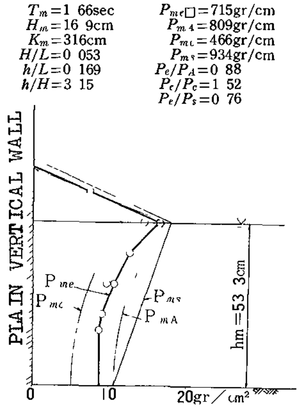

Fig. 3(a).

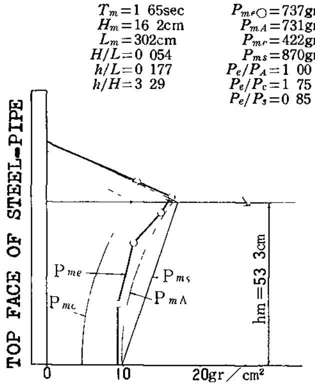

Fig. 4(a).

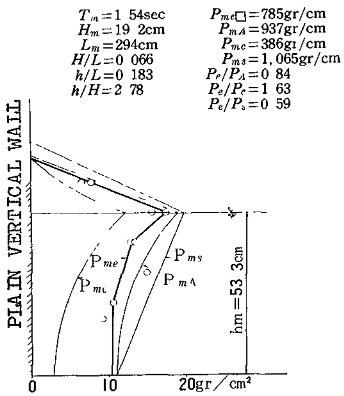

Fig. 5(a).

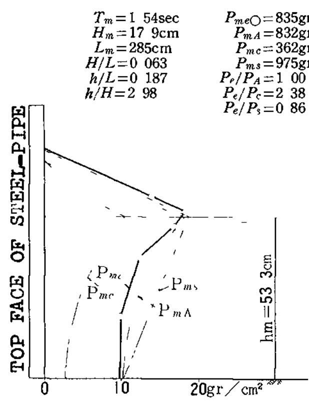

Fig. 6(a).

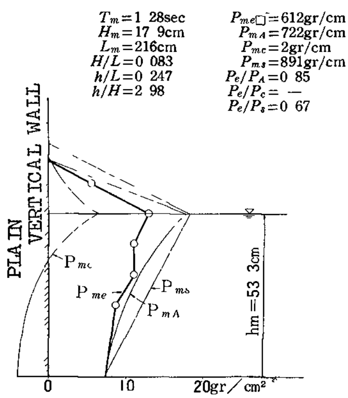

Fig. 7(a).

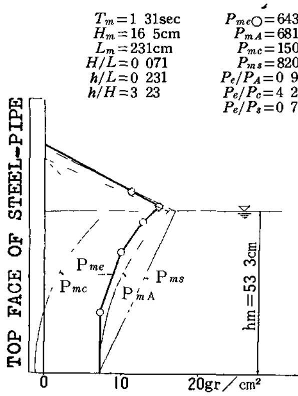

Fig. 8(a).

Figs. 3(a) - 7(a). Vertical distributions of wave pressures on the plain vertical wall.

Figs. 4(a) - 8(a). Vertical distributions of wave pressures on the steel-pipe breakwater.

$T_p = 6.5$sec $H_p = 2.4$m

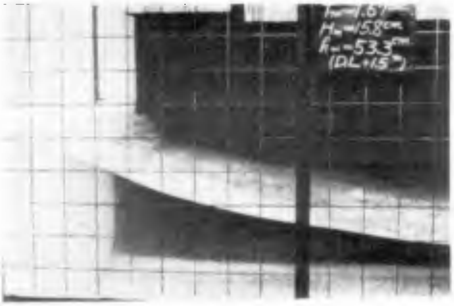

Fig. 3(b).

$T_p = 6.5$sec, $H_p = 2.4$m

Fig. 4(b).

$T_p = 6.0$sec, $H_p = 2.6$m

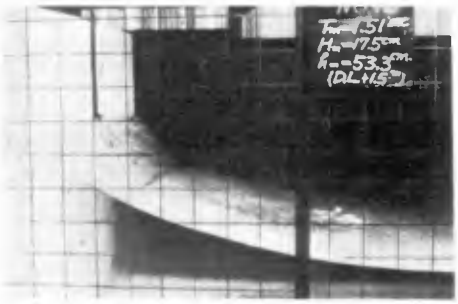

Fig. 5(b).

$T_p = 6.0$sec, $H_p = 2.6$m

Fig. 6(b).

$T_p = 5.0$sec. $H_p = 2.5$m

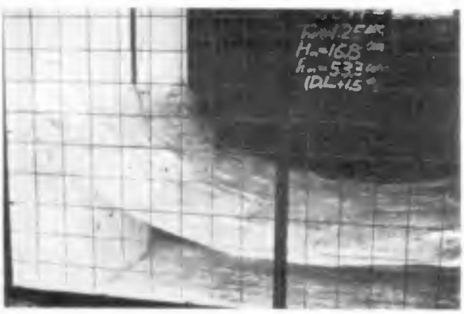

Fig. 7(b).

$T_p = 5.0$sec, $H_p = 2.5$m

Fig. 8(b).

Figs. 3(b) - 7(b). Behavior of wave in front of the plain vertical wall.

Figs. 4(b) - 8(b). Behavior of wave in front of the steel-pipe breakwater.

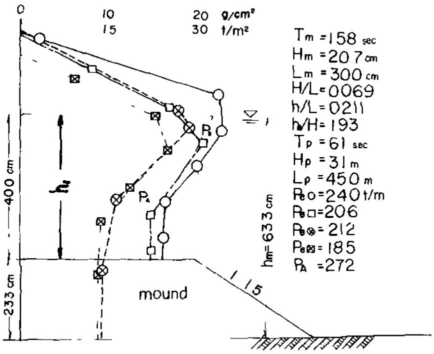

Fig. 9.

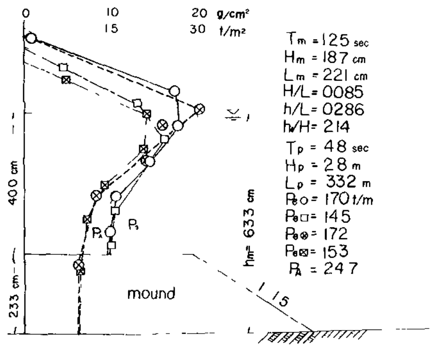

Fig. 10.

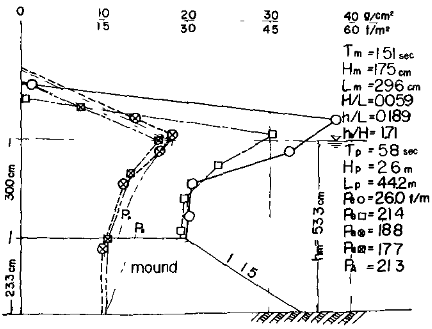

Fig. 11.

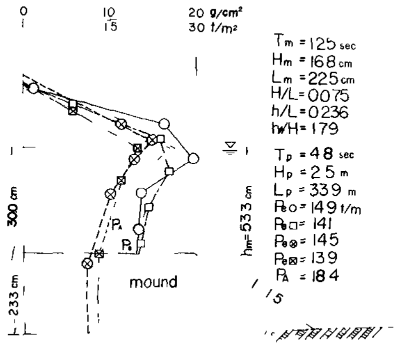

Fig. 12.

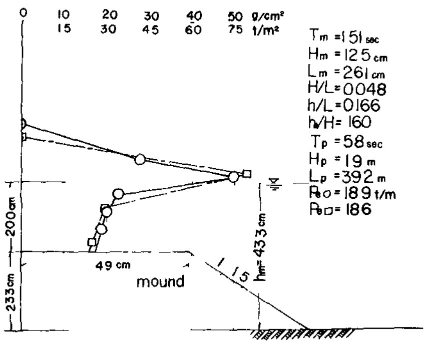

Fig. 13.

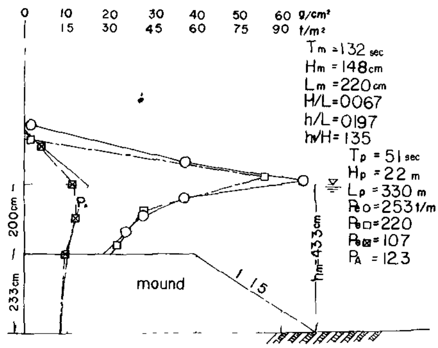

Fig. 14.

---⊗--- Steel Pipe without Base-Mound.

——⊙—— Steel Pipe with Base-Mound.

---⊠--- Plain Wall without Base-Mound.

——⊡—— Plain Wall with Base-Mound.

Fig. 9 - 14. Comparisons of the pressures on the steel-pipe breakwaters with and without a base-rubble mound.

Fig. 15.

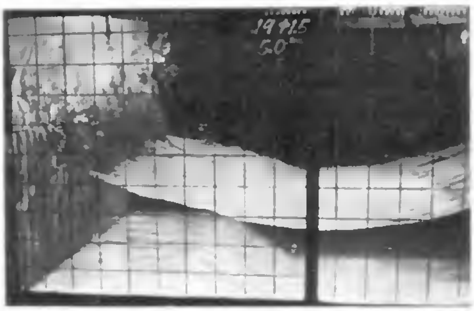

Fig. 16.

Fig. 17.

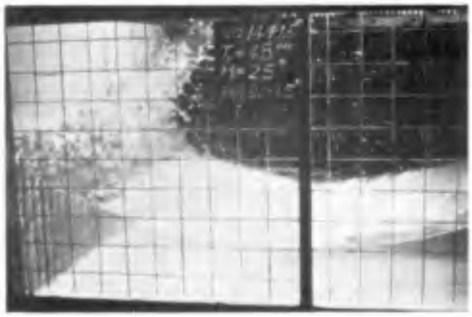

Fig. 18.

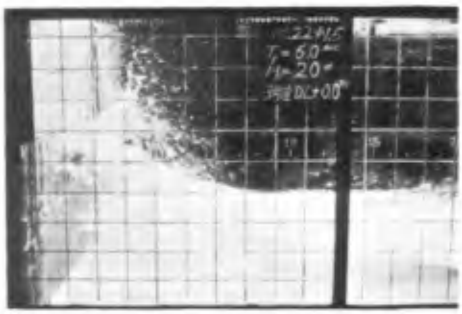

Fig. 19.

Fig. 20.

Figs. 15 - 20. Behavior of the wave in front of the steel-pipe breakwater with a rubble mound.

Fig. 21.

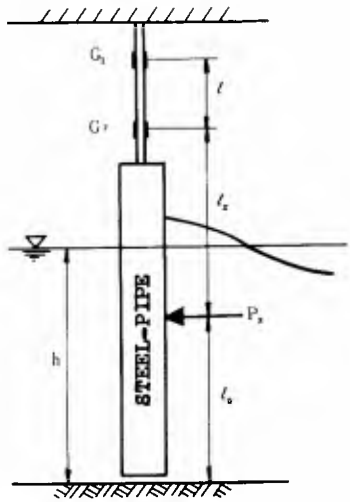

Fig. 22.

Figs. 21 - 22. Measurement of resultant pressure on one steel pipe by the moment method.

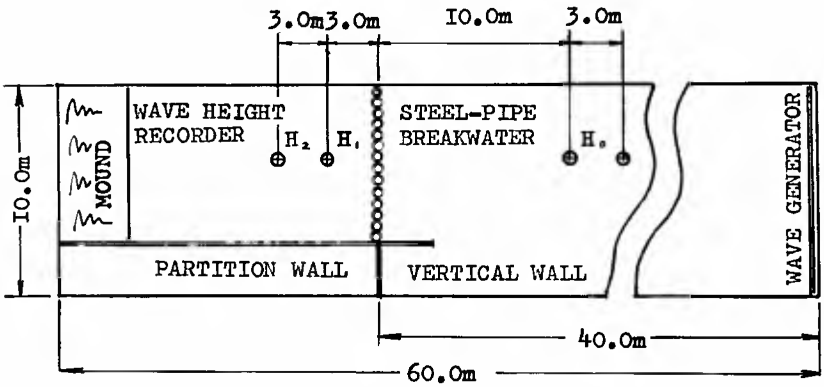

Fig. 23. Schematic layout of the experimental equipments in the wave tank.

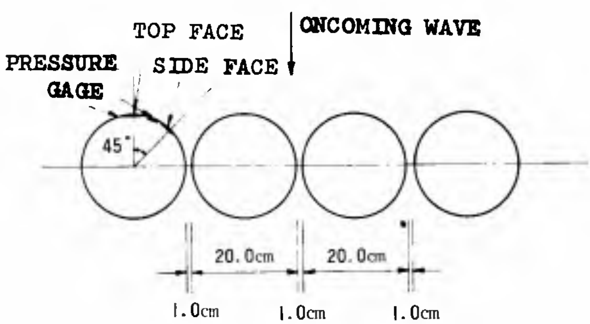

Fig. 24. Plan of the steel pipe breakwater.

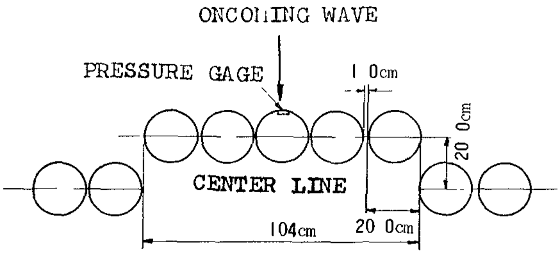

Fig. 25. Plan of the steel-pipe breakwater reconstructed after destruction.

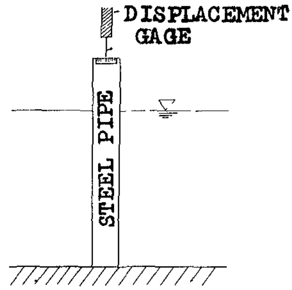

Fig. 26. Measurement of deflections at the top of the pipe.

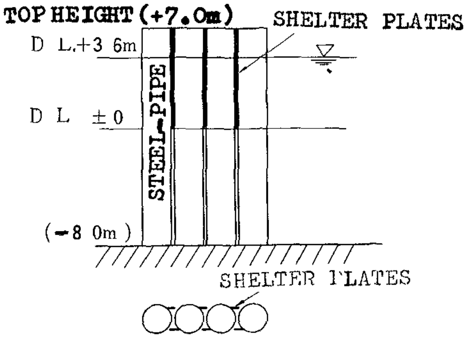

Fig. 27.

Iron plates welded to the pipes from L. W. L. to the top of the pipe.

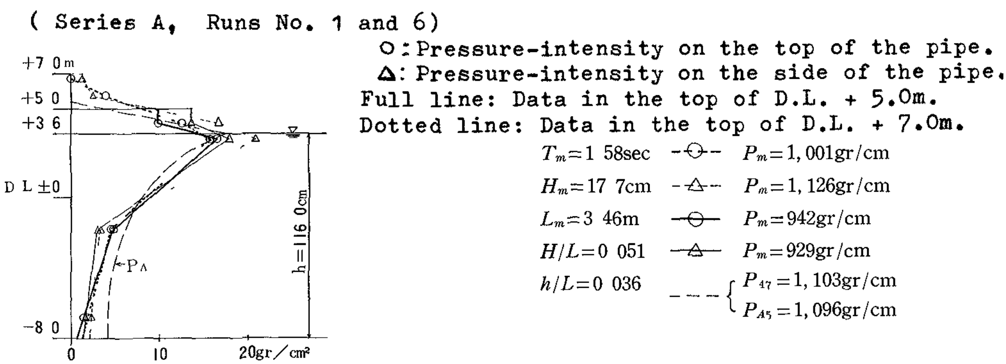

Fig. 28. Pressure distributions of the top face and the side of the steel-pipe breakwater.

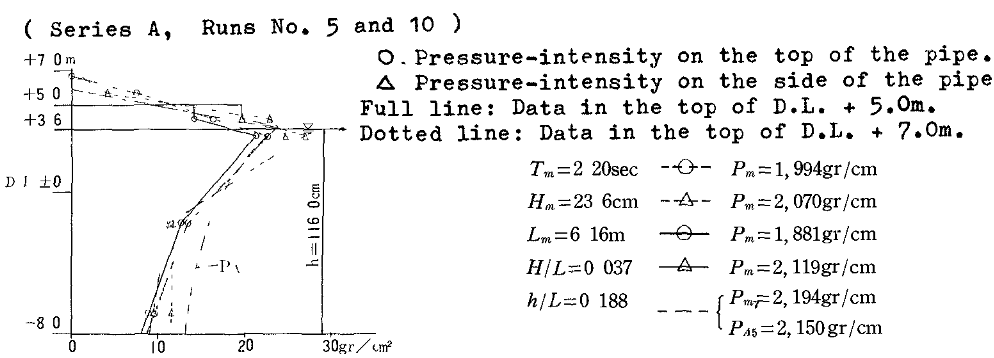

Fig. 29. Pressure distributions of the top face and the side of the steel-pipe breakwat

Table 5. Resultant of wave pressures on one steel pipe (Steel pipe breakwater without a rubble mound)

h_m (cm)	T_m (sec)	H_m (cm)	L_m (cm)	H/L	h/L
53.3	1.29	13.0	222	0.059	0.241
〃	1.31	16.5	231	0.071	0.231
〃	1.54	17.9	285	0.063	0.187
〃	1.65	16.2	302	0.054	0.187

h/H	P_{mA} (gr/cm)	P_{meO} (gr/cm)	l_{0O} (cm)	P_x (gr/本)	l_0 (cm)	$P_x / P_{meO} \times D_m$
4.10	604	481	37.1	5,890	43.0	1.23
3.23	681	643	37.9	7,360	38.2	1.15
2.98	832	835	37.2	9,400	41.0	1.13
3.29	731	737	35.8	8,970	39.0	1.22

P_x : Resultant pressure exerted on one pipe calculated by the moment method.
P_{meo}: Resultant pressure on the top face of the pipe.
D_m : Diameter of the pipe.

(a) Series A, Run No. 1. (b) Series A, Run No. 6.

Fig. 30. Behaviors of waves around the breakwater.

(a) Series A, Run No. 5. (b) Series A, Run No. 10.

Fig. 31. Behaviors of waves around the breakwater.

(Series C, Runs No. 3 and 6)

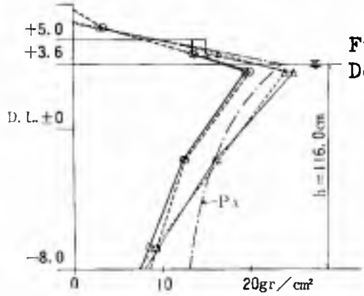

○: Pressure-intensity on the top of the pipe.
△: Pressure-intensity on the side of the pipe.
Full line: Data in the top of D.L. + 5.0m.
Dotted line: Data in the top of D.L. + 7.0m.

$T_m=2.20$sec —○— $P_m=1,788$gr/cm
$H_m=23.6$cm —△— $P_m=2,133$gr/cm
$L_m=6.16$m —○— $P_m=1,694$gr/cm
$H/L=0.037$ —△— $P_m=2,239$gr/cm
$h/L=0.188$ ——— { $P_{A7}=2,196$ gr/cm, $P_{A5}=2,150$ gr/cm }

Fig. 32. Pressure distributions of the top face and the side of the steel-pipe breakwater.

(a) Series C, Run No. 3.   (b) Series C, Run No. 6.

Fig. 33. Behaviors of waves around the breakwater.

(Series D, Run No. 1)

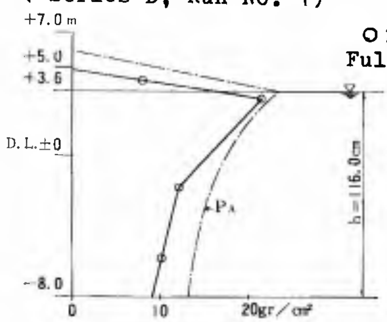

○: Pressure-intensity on the top of the pipe.
Full line: Data in the top of D.L. + 5.0m.

$T_m=1.58$sec
$H_m=22.3$cm
$L_m=3.65$m —○— $P_m=1,132$gr/cm
$H/L=0.061$
$h/L=0.318$ ——— $P_{A5}=1,464$ gr/cm

(a) Series D, Run No. 1.

Fig. 34. Experiments concerned with the reconstructed part.

(Series D, Run No. 2)

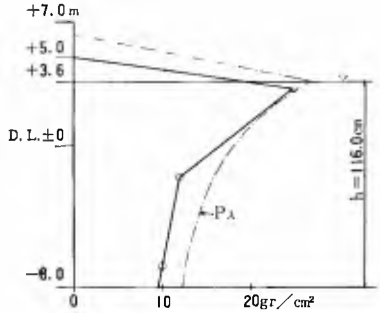

O : Pressure-intensity on the top of the pipe.
Full line: Data in the top of D.L. + 5.0m.

$T_m=1.93$sec
$H_m=26.7$cm
$L_m=5.13$m —⊖— $P_m=1,802$gr/cm
$H/L=0.052$
$h/L=0.226$ —·—·— $P_{A5}=2,216$gr/cm

(a) Series D, Run No. 2

Fig. 35. Experiments concerned with the reconstructed part.

Fig. 36. Steel-pipe breakwater in near completion in the Port of Osaka.

Fig. 37. Steel-pipe breakwater undergoing horizontal load tests.

Fig. 38. Steel-pipe breakwater after completion.

Fig. 39. Steel-pipe breakwater after completion.

Table 1. Comparison of the resultants of pressures between on the top face of the steel pipe and the plain vertical wall without rubble mound.

h_m (cm)	T_m (sec)	H_m (cm)	L_m (cm)	H/L	h/L	h/H	P_{mA} (gr/cm)	P_{mc} (gr/cm)	P_{ms} (gr/cm)	$P_{m\bigcirc}$ (gr/cm)	$P_{m\square}$ (gr/cm)	$P_{\bigcirc}/P_{\square}$	$P_{\square}/P_A$	$P_{\bigcirc}/P_A$
63.3	1.24	14.0	223	0.063	0.284	4.50	568	122	729	553	448	1.24	0.79	0.97
〃	1.27	18.3	248	0.074	0.255	3.46	833	97	1031	761	677	1.13	0.81	0.92
〃	1.53	18.8	319	0.059	0.198	3.36	987	297	1156	940	820	1.15	0.83	0.95
〃	1.52	16.8	312	0.054	0.203	3,76	854	423	985	762	684	1.12	0.80	0.89
〃	1.83	18.9	408	0.046	0.155	3.35	1,101	733	1,252	1,064	890	1.20	0.81	0.97
〃	2.03	16.2	430	0.038	0.147	3.95	945	706	1,051	974	850	1.15	0.90	1.03
53.3	1.31	16.5	231	0.071	0.231	3.23	631	150	820	643	612	1.05	0.90	0.94
〃	1,55	14.9	296	0.050	0.180	3.58	631	420	785	635	598	1.06	0.88	0.93
〃	1.54	17.9	285	0.063	0.187	2.93	832	352	975	835	785	1.06	0.94	1.00
〃	1.65	16.2	302	0.054	0.177	3.29	731	422	875	737	715	1.03	0.98	1.01

P_A : Resultant wave pressure calculated by the equation of maximum simultaneous pressure proposed by the author for standing waves in shallow water.
P_c : Resultant wave pressure calculated by the equation from the small amplitude wave theory.
P_s : Resultant wave pressure calculated by Sainflou's simplified method.
$P_{\bigcirc}$: Resultant wave pressure on the top face of the steel-pipe without a rubble mound.
$P_{\square}$: Resultant wave pressure on the plain vertical wall without a rubble mound.

Table 2. Comparison of the resultants of pressures between on the top face of the steel pipe and the plain vertical wall with rubble mound.

h_m (cm)	T_m (sec)	H_m (cm)	L_m (cm)	H/L	h/L	h_1/H	P_{mA} (gr/cm)	P_{mc} (gr/cm)	P_{ms} (gr/cm)	$P_{m\circledcirc}$ (gr/cm)	$P_{m\boxdot}$ (gr/cm)	$P_{\circledcirc}/P_{\boxdot}$	$P_{\boxdot}/P_A$	$P_{\circledcirc}/P_A$
63.3	1.24	14.0	223	0.063	0.284	2.86	510	153	592	506	451	1.12	0.89	0.99
〃	1.27	18.3	248	0.074	0.255	2.19	731	34	839	756	644	1.18	0.88	1.04
〃	1.53	18.8	319	0.059	0.198	2.13	806	274	884	1,065	911	1.17	1.13	1.32
〃	1.52	16.8	312	0.054	0.203	2.38	701	384	778	835	746	1.12	1.06	1.19
〃	1.83	18.9	403	0.046	0.155	2.12	853	589	943	1,042	830	1.26	0.97	1.22
53.3	1.29	13.0	221	0.059	0.240	2.31	402	164	440	453	417	1.09	1.10	1.13
〃	1.31	16.5	231	0.071	0.231	1.82	546	180	600	661	625	1.06	1.15	1.21
〃	1.55	14.9	296	0.050	0.180	2.01	509	328	534	1,154	849	1.36	1.67	2.27
〃	1.54	17.9	285	0.063	0.187	1.68	631	263	701	1,157	948	1.22	1.50	1.83
〃	1.65	16.2	302	0.054	0.177	2.04	559	286	613	745	653	1.14	1.17	1.34
43.3	1.32	14.8	220	0.067	0.197	1.35	—	—	—	1,125	976	1.15	—	—
〃	1.51	12.5	261	0.048	0.166	1.60	—	—	—	838	825	1.02	—	—

P_A : Resultant wave pressure calculated by the equation of maximum simultaneous pressure proposed by the author for standing waves in shallow water.
P_c : Resultant wave pressure calculated by the equation from the small amplitude wave theory.
P_s : Resultant wave pressure calculated Sainflou's simplified method.
$P_{\circledcirc}$: Resultant wave pressure on the top face of the steel-pipe with a rubble mound.
$P_{\boxdot}$: Resultant wave pressure on the plain vertical wall with a rubble mound.

Table 3. Comparison of wave pressures between on the top face and the side of the steel-pipe without a rubble mound.

h_m (cm)	T_m (sec)	H_m (cm)	L_m (cm)	H/L	h/L	h/H	P_{mA} (gr/cm)	$P_{me\triangle}$ (gr/cm)	$P_{m\bigcirc}$ (gr/cm)	$P_{\triangle}/P_{\bigcirc}$	$P_{\bigcirc}/P_A$
60 0	1 25	14 1	231	0 061	0 260	4 26	604	489	521	0 94	0 87
〃	1 27	17 3	242	0 072	0 248	3 47	760	644	646	1 00	0 85
〃	1 52	16 7	312	0 054	0 192	3 60	833	815	717	1 14	0 86
〃	1 55	18 0	318	0 057	0 189	3 34	918	858	796	1 08	0 87
〃	1 77	16 1	380	0 044	0 158	3 62	900	864	811	1 07	0 90

PA : Resultant wave pressure calculated by the equation of maximum simultaneous pressure proposed by the author for standing waves in shallow water.
Pc : Resultant wave pressure calculated by the equation from the small amplitude wave theory.
Ps : Resultant wave pressure calculated Sainflou's simplified method.
P△ : Resultant wave pressure on the side face of the steel-pipe without a rubble mound.

Table 4. Comparison of wave pressures between on the top face and the side of the steel-pipe with a rubble mound.

h_m (cm)	T_m (sec)	H_m (cm)	L_m (cm)	H/L	h/L	h/H	P_{mA} (gr/cm)	$P_{me\blacktriangle}$ (gr/cm)	$P_{me\circledcirc}$ (gr/cm)	$P_{\blacktriangle}/P_{\circledcirc}$
63 3	1 24	14 0	223	0 063	0 284	2 84	510	520	506	1 03
〃	1 27	18 3	248	0 074	0 255	2 19	731	803	756	1 06
〃	1 53	18 8	319	0 059	0 198	2 13	806	958	1,065	0 90
〃	1 52	16 8	312	0 054	0 203	2 38	701	745	835	0 89
〃	1 83	18 9	408	0 046	0 155	2 12	853	1,108	1,042	1 06

PA : Resultant wave pressure calculated by the equation of maximum simultaneous pressure proposed by the author for standing waves in shallow water.
Pc : Resultant wave pressure calculated by the equation from the small amplitude wave theory.
Ps : Resultant wave pressure calculated by Sainflou's simplified method.
P▲ : Resultant wave pressure on the side face of the steel-pipe with a rubble mound.

Table 7(a) Experimental results, Fixed top of the pipes with the shelter plates.

No	SERIES	TOP HEIGHTS (m)	h (cm) (m)	T_0 (sec) (sec)	L_0 (cm) (m)	H_0 (cm) (m)	H_0/L_0	h/L_0	P_A (gr/cm) (t/m)	$P_{\bigcirc}$ (gr/cm) (t/m)	$P_{\triangle}$ (gr/cm) (t/m)	$P_{\bigcirc}/P_A$	$P_{\triangle}/P_{\bigcirc}$	H_1 (cm)	H_2 (cm)	RATIO OF TRANSM (%) MEAS	RATIO OF TRANSM (%) CALCUL	OVERTOP.
1	A	5 0	116 (D L +3 6)	1 58 (5 00)	346 (34 6)	17 7 (1 77)	0 051	0 336	1,096 (10 96)	942 (9 42)	929 (9 29)	0 86	0 99	3 4	3 6	20	12	a little
2				1 58 (5 00)	365 (36 5)	22 3 (2 23)	0 061	0 318	1,464 (14 64)	1,168 (11 68)	1,351 (13 51)	0 80	1 16	4 1	4 3	19	13	compara. large
3				1 92 (6 08)	488 (48 8)	21 2 (2 12)	0 054	0 238	1,637 (16 37)	1,668 (16 68)	1,789 (17 89)	1 02	1 07	7 3	7 3	34	15	large
4				1 93 (6 12)	513 (51 3)	26 7 (2 67)	0 052	0 226	2,216 (22 16)	1,895 (18 95)	2,290 (22 90)	0 86	1 21	8 5	8 9	33	15	〃
5				2 20 (6 97)	616 (61 6)	23 6 (2 36)	0 037	0 188	2,150 (21 50)	1,881 (18 81)	2,119 (21 19)	0 87	1 13	7 9	8 1	34	16	〃
6		7 0		1 58 (5 00)	34、 (34 6)	17 7 (1 77)	0 051	0 336	1,103 (11 03)	1,001 (10 01)	1,126 (11 26)	0 91	1 13	3 1	3 1	18	12	null
7				1 58 (5 00)	365 (36 5)	22 3 (2 23)	0 061	0 318	1,498 (14 98)	1,363 (13 63)	1,570 (15 70)	0 71	1 15	4 2	4 3	19	13	〃
8				1 92 (6 08)	488 (48 8)	21 2 (2 12)	0 054	0 238	1,713 (17 13)	1,662 (16 62)	1,846 (18 46)	0 99	1 11	2 9	3 1	14	15	〃
9				1 93 (6 12)	513 (51 3)	26 7 (2 67)	0 052	0 226	2,297 (22 97)	1,990 (19 90)	2,273 (22 73)	0 87	1 14	4 0	4 0	15	15	〃
10				2 20 (6 97)	616 (61 6)	23 6 (2 36)	0 037	0 188	2,196 (21 96)	1,994 (19 94)	2,070 (20 70)	0 91	1 04	3 9	4 1	17	16	〃
11			97 (D L +1 7)	1 58 (5 00)	415 (41 5)	18 0 (1 80)	0 043	0 210	—	—	—	—	—	3 3	3 5	19	17	〃
12				1 80 (6 00)	546 (54 6)	22 0 (2 20)	0 040	0 177	—	—	—	—	—	4 3	4 5	20	18	〃

( ) indicates the corresponding values in prototype.

Table 7(b). Experimental results, movable top of the pipe with shelter plates.

No	SERIES	TOP HEIGHTS (m)	h (cm) (m)	T_0 (sec) (sec)	L_0 (cm) (m)	H_0 (cm) (m)	H_0/L_0	h/L_0	P_A (gr/cm) (t/m)	$P_○$ (gr/cm) (t/m)	$P_△$ (gr/cm) (t/m)	$P_○/P_A$	$P_△/P_○$	H_t (cm)	H (cm)
1	B	5 0	116 (D L +3 6)	1 58 (5 00)	346 (34 6)	17 7 (1 77)	0 051	0 336	1,096 (10 96)	1,129 (11 29)	1,863 (18 63)	1 03	1 65	—	—
2				1 58 (5 00)	365 (36 5)	22 3 (2 23)	0 061	0 318	1,464 (14 64)	923 (9 23)	1,743 (17 43)	0 63	1 89	—	—
3				1 92 (6 08)	488 (48 8)	21 2 (2 12)	0 054	0 238	1,637 (16 37)	1,309 (13 09)	2,318 (23 18)	0 80	1 77	—	—
4				1 93 (6 12)	513 (51 3)	26 7 (2 67)	0 052	0 226	2,216 (22 16)	1,721 (17 21)	2,370 (23 70)	0 78	1 38	—	—
5				2 20 (6 97)	615 (61 5)	23 6 (2 36)	0 037	0 188	2,150 (21 50)	1,841 (18 41)	2,430 (24 30)	0 86	1 32	—	—
6		7 0		1 58 (5 00)	346 (34 6)	17 7 (1 77)	0 051	0 336	1,103 (11 03)	1,191 (11 91)	1,550 (15 50)	1 08	1 30	—	—
7				1 58 (5 00)	365 (36 5)	22 3 (2 23)	0 061	0 318	1,498 (14 98)	1,177 (11 77)	2,183 (21 83)	0 79	1 82	—	—
8				1 92 (6 08)	488 (48 8)	21 2 (2 12)	0 054	0 238	1,713 (17 13)	1,746 (17 46)	2,591 (25 91)	1 02	1 48	—	—
9				1 93 (6 12)	513 (51 3)	26 7 (2 67)	0 052	0 226	2,297 (22 97)	1,924 (19 24)	2,281 (22 81)	0 84	1 19	—	—
10				2 20 (6 97)	616 (61 6)	23 6 (2 36)	0 037	0 188	2,196 (21 96)	1,746 (17 46)	2,431 (24 31)	0 80	1 39	—	—

( ) indicates the corresponding values in prototype.

Table 6. Kinds of experiments conducted.

SERIES	RATIO OF SPACES α (%)	SHELTER PLATES	DIFLECT OF THE TOP (cm)	WATER LEVEL D L +(m)	TOP HEIGHTS D L +(m)	OBJECT OF EXPER.	REFERENCE
A	5	with	0	3 6 1 7	5 0 7 0 7 0	wave pressure ratio of transm. ratio of transm.	Table 7(a)
B	5	with	2 0	3 6	5 0 7 0	wave pressure	Table 7(b)
C	5	without	0	3 6 1 7 1 1	5 0 7 0 5 0 5 0	wave pressure ratio of transm. ratio of transm. "	Table 7(c)
D	5	without	0	3 6	5 0	wave pressure ratio of transm.	
E	5	without	7 0	3 6	7 0	ratio of transm	

α : Ratio of spaces between the pipes against the diameter of pipe.

$\alpha = d/D$

Table 7(c) Experimental results, Fixed top of the pipes without the shelter plates.

No	SERIES	TOP HEIGHTS (m)	h (cm) (m)	T_0 (sec) (sec)	L_0 (cm) (m)	H_0 (cm) (m)	H_0/L_0	h/L_0	P_4 (gr/cm) (t/m)	$P_○$ (gr/cm) (t/m)	$P_△$ (gr/cm) (t/m)	$P_○/P_4$	$P_△/P_○$	H_1 (cm)	H_2 (cm)	RATIO OF TRANSM. (%) MEAS.	RATIO OF TRANSM. (%) CALCUL.	OVERTOP.
1	C	5 0	116 (D L +3 6)	1 58 (5 00)	365 (36 5)	22 3 (2 23)	0 061	0 318	1, 464 (14 64)	1, 039 (10 39)	1, 405 (14 05)	0 71	1 35	9 3	9 4	42	22	compara. large
2				1 93 (6 12)	513 (51 3)	26 7 (2 67)	0 052	0 226	2, 216 (22 16)	1, 561 (15 61)	2, 221 (22 21)	0 70	1 42	11 4	11 6	43	22	large
3				2 20 (6 97)	616 (61 6)	23 6 (2 36)	0 037	0 188	2, 150 (21 50)	1, 694 (16 94)	2, 239 (22 39)	0 79	1 32	9 9	9 9	42	22	compara. large
4		7 0		1 58 (5 00)	365 (36 5)	22 3 (2 23)	0 061	0 318	1, 498 (14 98)	1, 078 (10 78)	1, 333 (13 33)	0 72	1 24	6 2	6 3	28	22	null
5				1 93 (6 12)	513 (51 3)	26 7 (2 67)	0 052	0 226	2, 297 (22 97)	1, 728 (17 28)	2, 165 (21 65)	0 75	1 25	7 9	8 1	30	22	〃
6				2 20 (6 97)	616 (61 6)	23 6 (2 36)	0 037	0 188	2, 196 (21 96)	1, 788 (17 88)	2, 133 (21 33)	0 81	1 19	6 5	6 7	28	22	〃
7		5 0	97 (D L +1 7)	1 58 (5 00)	415 (41 5)	21 0 (2 10)	0 051	0 210	—	—	—	—	—	6 1	6 1	29	22	〃
8				1 80 (6 00)	546 (54 6)	23 0 (2 30)	0 040	0 177	—	—	—	—	—	7 5	7 7	33	22	〃
9				2 22 (7 00)	652 (65 2)	18 0 (1 80)	0 028	0 149	—	—	—	—	—	5 0	5 1	28	22	〃
10			91 (D L +1 1)	2 22 (7 00)	652 (65 2)	15 0 (1 50)	0 023	0 140	—	—	—	—	—	4 9	5 0	33	22	〃

( ) indicates the corresponding values in prototype.